

Two-pion contributions to the muon $g - 2$

Peter Stoffer*

Department of Physics, University of California at San Diego, La Jolla, CA 92093, USA

E-mail: pstoffer@ucsd.edu

Gilberto Colangelo

Albert Einstein Center for Fundamental Physics, Institute for Theoretical Physics,

University of Bern, Sidlerstrasse 5, 3012 Bern, Switzerland

E-mail: gilberto@itp.unibe.ch

Martin Hoferichter

Institute for Nuclear Theory, University of Washington, Seattle, WA 98195-1550, USA

E-mail: mhofer@uw.edu

We perform a detailed analysis of $e^+e^- \rightarrow \pi^+\pi^-$ data for energies below 1 GeV, based on a dispersive representation of the pion vector form factor. Using an extended Omnès representation and input for the $\pi\pi$ P -wave phase shift from a previous Roy-equation analysis, we express the pion vector form factor in terms of a few free parameters, which are fit to the modern high-statistics data sets. Statistically acceptable fits are obtained as soon as potential uncertainties in the energy calibration are taken into account. The fits prefer a mass of the ω meson significantly lower than the current PDG average. We perform a complete analysis of statistical and systematic uncertainties and derive the consequences for the two-pion contribution to hadronic vacuum polarization and the muon anomalous magnetic moment a_μ . In a global fit, we find $a_\mu^{\pi\pi}|_{\leq 1\text{GeV}} = 495.0(1.5)(2.1) \times 10^{-10}$ and $a_\mu^{\pi\pi}|_{\leq 0.63\text{GeV}} = 132.8(0.4)(1.0) \times 10^{-10}$. As side products, we obtain improved constraints on the $\pi\pi$ P -wave as well as a determination of the pion charge radius, $\langle r_\pi^2 \rangle = 0.429(1)(4) \text{fm}^2$.

*The 9th International workshop on Chiral Dynamics
17–21 September 2018
Durham, NC, USA*

*Speaker.

1. Introduction

Hadronic vacuum polarization (HVP) is the dominant hadronic contribution to the anomalous magnetic moment of the muon a_μ [1–3]. About 70% of this contribution is due to the two-pion channel, which is also responsible for a similar fraction of the uncertainty of the HVP contribution to a_μ . Unitarity relates this contribution to the pion vector form factor (VFF) F_π^V , which is accessible in the reaction $e^+e^- \rightarrow \pi^+\pi^-$.

Unitarity and analyticity of the VFF itself allow one to express this object in terms of the $\pi\pi$ scattering phase shift, up to inelastic corrections. Very precise representations of the elastic $\pi\pi$ phase shifts up to roughly 1 GeV have been obtained in analyses [4–6] of the Roy equations [7].

Dispersion relations that connect the two-pion HVP contribution to a_μ with the pion VFF and $\pi\pi$ scattering have been established long ago [8–11]. Similar representations have been used more recently [12–15], in particular in the context of our dispersive approach to hadronic light-by-light (HLbL) scattering [16–23]. At this conference, the two-pion contributions to HLbL were presented in [24].

In the last two decades, the experimental situation in $e^+e^- \rightarrow \pi^+\pi^-$ has improved considerably, but at the same time the required precision of the HVP contribution to a_μ has increased further, in particular in view of the anticipated improvement of the experimental measurement of a_μ by a factor 4 at the Fermilab experiment. Most current HVP compilations are based on a direct integration of the experimental data [25–27], wherein conflicting data sets are treated by a local χ^2 inflation. The most consequential such tensions currently affect the BaBar [28, 29] and KLOE [30–33] data sets for the $\pi\pi$ channel, and different methods for their combination then give rise to the single largest difference between the HVP compilations of [26] and [27].

Here, we summarize our recent reanalysis of the $\pi\pi$ contribution to HVP based on a dispersive representation of the VFF [34]. We explain the global fit function that the VFF needs to follow to avoid conflicts with unitarity and analyticity. The resulting representation is fit to the modern high-statistics data sets, by using an unbiased fit strategy and including the full experimental covariance matrices where available, providing a strong check of the internal consistency of each data set. We address the systematic uncertainties in the dispersive representation and derive the HVP results for various energy intervals. As side products, we obtain improved constraints on the $\pi\pi$ P -wave phase shift as well as a determination of the pion charge radius.

2. Dispersive representation of the pion vector form factor

In the following, we give a short summary of the dispersive representation of the pion VFF $F_\pi^V(s)$ as put forward in [9, 10]. The VFF is related to the final-state-radiation-inclusive cross section by

$$\sigma(e^+e^- \rightarrow \gamma^* \rightarrow \pi^+\pi^-(\gamma)) = \left[1 + \frac{\alpha}{\pi}\eta(s)\right] \frac{\pi|\alpha(s)|^2}{3s} \sigma_\pi^3(s) |F_\pi^V(s)|^2 \frac{s + 2m_e^2}{s\sigma_e(s)}, \quad (2.1)$$

where the effect of vacuum polarization is expressed in terms of the running coupling $\alpha(s)$ and $\eta(s)$ describes the final-state radiation within scalar QED [35–37]. The correction of initial-state radiation is performed with Monte Carlo generators in the context of each experiment [38–40, 36].

In order to apply the constraints of unitarity and analyticity, we need to treat the form factor in pure QCD. We include the most important strong isospin-breaking effect from the mixing into the 3π channel. For a more detailed discussion of radiative corrections, we refer to [34].

In the isospin limit, $F_\pi^V(s)$ is an analytic function of s , apart from a branch cut in the complex s -plane that lies on the real axis, $s \in [4M_\pi^2, \infty)$, and is dictated by unitarity. We parametrize the pion VFF as a product of three functions,

$$F_\pi^V(s) = \Omega_1^1(s) G_\omega(s) G_{\text{in}}^N(s), \quad (2.2)$$

where

$$\Omega_1^1(s) = \exp \left\{ \frac{s}{\pi} \int_{4M_\pi^2}^{\infty} ds' \frac{\delta_1^1(s')}{s'(s'-s)} \right\} \quad (2.3)$$

is the usual Omnès function [41] with $\delta_1^1(s)$ the isospin $I = 1$ elastic $\pi\pi$ phase shift in the isospin-symmetric limit. The factor G_ω accounts for ρ - ω mixing, the most important isospin-breaking effect, which becomes enhanced by the small mass difference between the ρ and ω resonances. The parametrization

$$G_\omega(s) = 1 + \frac{s}{\pi} \int_{9M_\pi^2}^{\infty} ds' \frac{\text{Im } g_\omega(s')}{s'(s'-s)} \left(\frac{1 - \frac{9M_\pi^2}{s'}}{1 - \frac{9M_\pi^2}{M_\omega^2}} \right)^4, \quad g_\omega(s) = 1 + \epsilon_\omega \frac{s}{(M_\omega - \frac{i}{2}\Gamma_\omega)^2 - s} \quad (2.4)$$

implements the correct threshold behavior of the discontinuity, i.e. the right-hand cut starting at $9M_\pi^2$ opens with the fourth power of the center-of-mass momentum [9]. The remaining function $G_{\text{in}}^N(s)$ is analytic in the complex s -plane with a cut on the real axis starting at $s = 16M_\pi^2$. It takes into account all further inelastic contributions to the unitarity relation. We describe it by a conformal polynomial

$$G_{\text{in}}^N(s) = 1 + \sum_{k=1}^N c_k (z^k(s) - z^k(0)), \quad z(s) = \frac{\sqrt{s_{\text{in}} - s_c} - \sqrt{s_{\text{in}} - s}}{\sqrt{s_{\text{in}} - s_c} + \sqrt{s_{\text{in}} - s}} \quad (2.5)$$

and we consider inelasticities only above $s_{\text{in}} = (M_{\pi^0} + M_\omega)^2$, since 4π inelasticities are extremely weak below. P -wave behavior at the inelastic threshold requires

$$c_1 = - \sum_{k=2}^N k c_k. \quad (2.6)$$

This parametrization of the VFF fulfills all requirements of analyticity and unitarity, including explicitly the 2π and 3π channels and inelastic corrections in the conformal polynomial. We expect this representation to be accurate as long as the conformal polynomial provides an efficient description of inelastic effects, conservatively estimated below $\sqrt{s} = 1 \text{ GeV}$. As main input, we require the elastic $\pi\pi$ P -wave phase shift $\delta_1^1(s)$. The isospin-breaking corrections are parametrized in terms of the ω parameters ϵ_ω , M_ω , and Γ_ω . The inelastic contribution is parametrized in terms of $N - 1$ free parameters c_k as well as s_c , the point that is mapped to the origin $z(s_c) = 0$ and should be chosen sufficiently far below any thresholds.

The input for the elastic P -wave $\pi\pi$ scattering phase shift is taken from the solution of the Roy-equation analysis [4, 6]. This solution depends on 27 parameters, which we treat as a source of systematic uncertainties, apart from two parameters that represent the values of the P -wave phase shift at $s_0 = (0.8 \text{ GeV})^2$ and at $s_1 = (1.15 \text{ GeV})^2$. They were estimated in [6] as

$$\delta_1^1(s_0) = 108.9(2.0)^\circ, \quad \delta_1^1(s_1) = 166.5(2.0)^\circ. \quad (2.7)$$

In our description of the VFF, we do not use these estimates but treat the values of the phase at s_0 and s_1 as free fit parameters. At energies above 1.3 GeV , the $\pi\pi$ phase shift is not as well known as in the low-energy region and represents another source of systematic uncertainty, which we estimate by considering different continuations to an asymptotic value $\lim_{s \rightarrow \infty} \delta_1^1(s) = \pi$.

In [42, 43], a generalization of Watson's theorem [44] was derived that amounts to a constraint on the difference between the phase of the VFF and the elastic $\pi\pi$ scattering phase shift, the Eidelman–Łukaszuk (EŁ) bound. With data input on the ratio of non- 2π to 2π hadronic cross sections in the isospin $I = 1$ channel [43], the EŁ bound provides an important constraint on the parameters c_k of the conformal polynomial that we use to describe the inelastic contributions.

3. Fits to e^+e^- data

The dispersive representation of the VFF is fit to modern high-statistics e^+e^- data sets. We take into account the results from the energy-scan experiments SND [45, 46] and CMD-2 [47–50] as well as from the radiative-return experiments BaBar [28, 29] and KLOE [30–33]. In addition to these time-like data sets, we use NA7 data [51] on the space-like form factor from the scattering of pions off an electron target. Where available, we use the full experimental covariance matrices and treat systematic errors with the iterative method proposed by the NNPDF collaboration [52], which avoids the D'Agostini bias [53].

We find that statistically acceptable fits to each experiment separately are possible, provided that the distinct ρ - ω interference shape in the data is properly aligned with the fit function. This requires either the ω mass to be taken as a free fit parameter or a rescaling of the energies of the data points, reflecting a possible experimental calibration uncertainty. We perform fits to combinations of experiments and in this case both allow the ω mass to float and include an energy rescaling in each experiment, constrained by the experimental calibration uncertainties.

We observe that in the KLOE data set, two data points are responsible for a contribution of more than 30 units to the χ^2 of our fits. Removing these two points as obvious outliers improves the goodness of the fit without significantly changing the central values of the fit results.

As shown in Fig. 1, both our final result for the ω mass resulting from the fit to the combination of all experiments

$$M_\omega = 781.68(9)(3) \text{ MeV}, \quad (3.1)$$

and the results from fits to single experiments disagree with the PDG average, which is mainly based on $e^+e^- \rightarrow 3\pi$ data [54, 48]. This observation has been made before [29, 15] and deserves further attention.

In Table 1, we show the fit results to single time-like data sets. The parameters ξ_j denote the applied energy rescaling of the data points and KLOE'' denotes the data set where the two

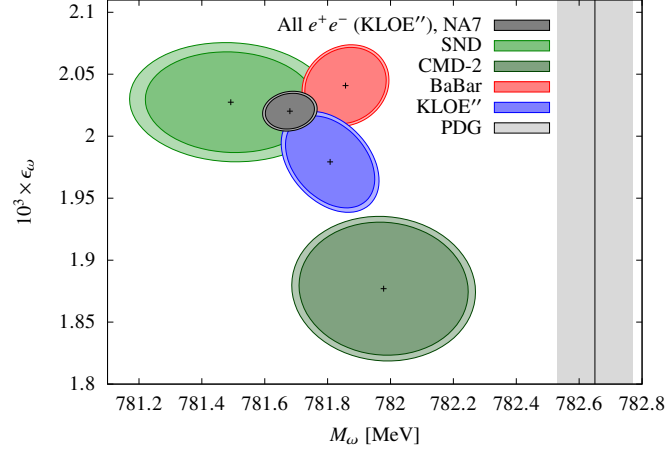


Figure 1: Error ellipses for the parameters ϵ_ω and M_ω resulting from fits to single experiments and the fit to the combination of all experiments. The smaller ellipses are standard error ellipses that correspond to $\Delta\chi^2 = 1$, the larger ellipses are inflated by the PDG scale factor $S = \sqrt{\chi^2/\text{dof}}$.

	χ^2/dof	M_ω [MeV]	$10^3 \times \xi_j$	$\delta_1^1(s_0)$ [°]	$\delta_1^1(s_1)$ [°]	$10^3 \times \epsilon_\omega$
SND	51.9/37 = 1.40	781.49(32)(2)	0.0(6)(0)	110.5(5)(8)	165.7(0.3)(2.4)	2.03(5)(2)
CMD-2	87.4/74 = 1.18	781.98(29)(1)	0.0(6)(0)	110.5(5)(8)	166.4(0.4)(2.4)	1.88(6)(2)
BaBar	299.1/262 = 1.14	781.86(14)(1)	0.0(2)(0)	110.4(3)(7)	165.7(0.2)(2.5)	2.04(3)(2)
KLOE	254.5/187 = 1.36	781.82(17)(4)	$\begin{cases} 0.6(2)(0) \\ -0.3(2)(0) \\ -0.2(3)(0) \end{cases}$	110.4(2)(6)	165.6(0.1)(2.4)	1.97(4)(2)
KLOE''	222.5/185 = 1.20	781.81(16)(3)	$\begin{cases} 0.5(2)(0) \\ -0.3(2)(0) \\ -0.2(3)(0) \end{cases}$	110.3(2)(6)	165.6(0.1)(2.4)	1.98(4)(1)

Table 1: Final fits to single e^+e^- experiments with $N - 1 = 4$ free parameters in the conformal polynomial. The first error is the fit uncertainty, inflated by $\sqrt{\chi^2/\text{dof}}$, the second error is the combination of all systematic uncertainties.

outliers are removed. The fit quality corresponds to p -values between 3% and 14%, apart from the fit to KLOE including the two outliers (with a p -value of 7×10^{-4}). Detailed results for the fits to combinations of data sets including the space-like NA7 data can be found in [34].

Fig. 2 shows the result for the pion VFF in the region of the ρ - ω interference in a fit to the combination of all experiments. Fig. 3 shows the relative difference between the data points and the fit in the energy region $[0.6, 0.9]$ GeV. The well-known discrepancy between the BaBar and KLOE data sets is evident. In all results, the fit errors are inflated by a scale factor [55] $S = \sqrt{\chi^2/\text{dof}}$, which in fits to combinations of data sets lies between 1.12 and 1.19. We remark that in particular for high statistics, this prescription does not fully account for a situation where the systematic uncertainties in the experiments were underestimated.

4. Contribution to the anomalous magnetic moment of the muon

In Table 2 we collect the results for $a_\mu^{\pi\pi}$ for single time-like experiments and a variety of different energy regions below 1 GeV, some of which have been considered in previous work.

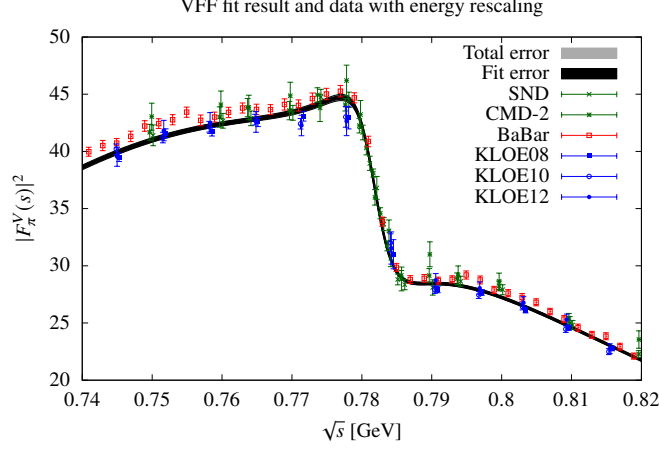


Figure 2: Fit result for the pion VFF in the ρ - ω interference region, together with the e^+e^- data sets. The data points are shown with the energy rescaling and the curve is the fit result with (3.1) for the ω mass.

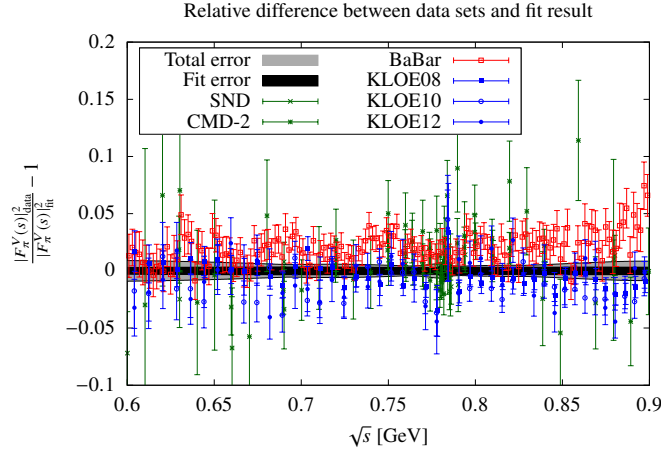


Figure 3: Relative difference between the data points and the fit result for the VFF, normalized to the fit result for $|F_\pi^V(s)|^2$. The total error is given by the fit error and the systematic uncertainty, added in quadrature.

Fig. 4 illustrates the results for $a_\mu^{\pi\pi}$ below 1 GeV including fits to the combination of the energy-scan experiments SND and CMD-2, all time-like data sets, and the full combination including NA7. More detailed results for the fits to the combination of experiments are given in [34].

Where published results are available, we have included the comparison in the tables, e.g. from direct integration [33, 27] and the dispersive analysis [13]. We find that our results are well compatible, within uncertainties of a similar size. An exception is the comparison to the direct integration of the data between $\sqrt{0.1}$ and $\sqrt{0.95}$ GeV performed by KLOE [33] where our method shows a significant reduction of the uncertainties: this is mainly due to the region below 0.6 GeV where KLOE data show a loss of precision. In the regions where there are high-quality data, these are so precise and densely spaced that our method mainly serves as a check of the consistency of the data with the principles of analyticity and unitarity. We stress that our uncertainty estimates rely on minimal assumptions, the dispersive parametrization as a consequence of QCD and the covariances matrices provided by experiment.

Our most comprehensive result gives the full contribution below 1 GeV in a combination of all

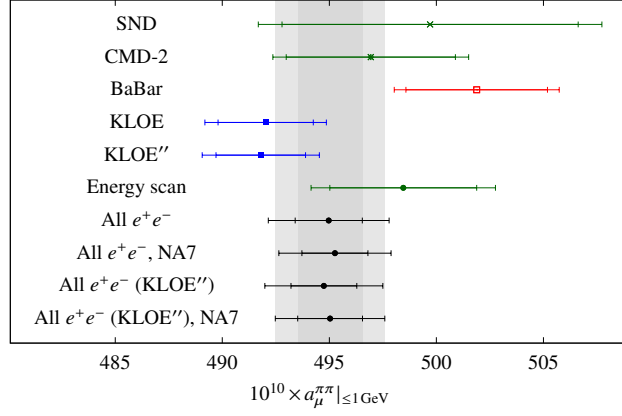
Result for $a_\mu^{\pi\pi}|_{\leq 1\text{GeV}}$ from the VFF fits to single experiments and combinations

Figure 4: Results for $a_\mu^{\pi\pi}$ in the energy range ≤ 1 GeV. The smaller error bars are the fit uncertainties, inflated by $\sqrt{\chi^2/\text{dof}}$, the larger error bars are the total uncertainties. The gray bands indicate our final result.

$10^{10} \times a_\mu^{\pi\pi}$ Energy region [GeV]	≤ 0.6	≤ 0.7	≤ 0.8	≤ 0.9	≤ 1.0
SND	110.3(1.2)(1.4)	215.8(2.9)(2.5)	416.3(5.7)(3.6)	484.0(6.7)(4.0)	499.7(6.9)(4.1)
CMD-2	109.1(1.0)(1.3)	212.8(2.1)(2.1)	413.2(3.4)(2.1)	481.4(3.9)(2.3)	496.9(4.0)(2.3)
BaBar	110.8(6)(8)	216.8(1.4)(1.3)	418.2(2.8)(1.8)	486.1(3.2)(2.0)	501.9(3.3)(2.0)
KLOE	110.1(5)(5)	214.6(1.1)(1.2)	411.2(1.9)(1.6)	477.0(2.2)(1.8)	492.0(2.2)(1.8)
KLOE''	110.2(5)(5)	214.6(1.0)(1.0)	410.9(1.8)(1.4)	476.7(2.0)(1.7)	491.8(2.1)(1.8)
Energy region [GeV]	≤ 0.63	[0.6, 0.9]	Ref. [33]	$[\sqrt{0.1}, \sqrt{0.95}]$	Ref. [33]
SND	133.2(1.6)(1.7)	373.6(5.6)(2.6)	371.7(5.0)	495.3(6.9)(4.0)	
CMD-2	131.6(1.2)(1.6)	372.2(3.1)(1.0)	372.4(3.0)	492.6(3.9)(2.3)	
BaBar	133.8(8)(9)	375.3(2.7)(1.2)	376.7(2.7)	497.5(3.3)(2.0)	
KLOE	132.8(6)(8)	366.8(1.8)(1.5)	366.9(2.1)	487.7(2.2)(1.8)	489.8(5.1)
KLOE''	132.9(6)(6)	366.5(1.7)(1.6)	366.9(2.1)	487.5(2.1)(1.7)	489.8(5.1)

Table 2: Values for $a_\mu^{\pi\pi}$ from our final fits to single e^+e^- experiments. The first error is the fit uncertainty, inflated by $\sqrt{\chi^2/\text{dof}}$, the second error the combination of all systematic uncertainties. The energy regions in the second block are provided to facilitate comparison with [13] and the results of the direct integration [33].

available time- and space-like constraints

$$a_\mu^{\pi\pi}|_{\leq 1\text{GeV}} = 495.0(1.5)(2.1) \times 10^{-10} = 495.0(2.6) \times 10^{-10}, \quad (4.1)$$

where the inclusion of the space-like data does allow for a modest reduction of the uncertainty from 2.8 to 2.6 units. As noted before [13], the main advantage over direct integration occurs in energy regions where data are still scarce, most notably the low-energy region

$$a_\mu^{\pi\pi}|_{\leq 0.63\text{GeV}} = 132.8(0.4)(1.0) \times 10^{-10} = 132.8(1.1) \times 10^{-10}. \quad (4.2)$$

Our result agrees with the combination of e^+e^- data sets from [13, 56], $a_\mu^{\pi\pi}|_{\leq 0.63\text{GeV}} = 132.9(8) \times 10^{-10}$, which provides another important cross check given several conceptual differences compared to our study.

5. Charge radius of the pion

The charge radius of the pion, $\langle r_\pi^2 \rangle$, is defined by the derivative of the VFF at $s = 0$

$$\langle r_\pi^2 \rangle = 6 \frac{dF_\pi^V(s)}{ds} \Big|_{s=0} = \frac{6}{\pi} \int_{4M_\pi^2}^{\infty} ds \frac{\text{Im} F_\pi^V(s)}{s^2}. \quad (5.1)$$

With the VFF determined from the fit to $e^+e^- \rightarrow \pi^+\pi^-$ and space-like data sets, the dispersive integral produces the results

$$\langle r_\pi^2 \rangle = 0.429(1)(4) \text{ fm}^2 = 0.429(4) \text{ fm}^2. \quad (5.2)$$

The uncertainties are dominated by the variation of the order of the conformal polynomial N . In particular, in contrast to the HVP contribution, the sum rule (5.1) is directly sensitive to the phase of the conformal polynomial, which is only constrained by the E \mathbb{L} bound up to 1.15 GeV.

Within uncertainties, our result is consistent with the previous dispersive extraction $\langle r_\pi^2 \rangle = 0.432(4) \text{ fm}^2$ from [57], but the tension with the PDG average $\langle r_\pi^2 \rangle = 0.452(11) \text{ fm}^2$ [55] is further exacerbated. However, as noted before [15], this average does not contain any modern $e^+e^- \rightarrow \pi^+\pi^-$ data sets and, if potentially model-dependent extractions from $eN \rightarrow e\pi N$ [58, 59] were excluded, would be dominated by NA7 $\langle r_\pi^2 \rangle = 0.439(8) \text{ fm}^2$ [51], in better agreement with (5.2).

6. Conclusions

We analyzed the strong constraints of analyticity and unitarity on $\pi\pi$ scattering and the pion VFF and worked out in detail the consequences for the HVP contribution to the anomalous magnetic moment of the muon, including a consistent implementation of all uncertainties. The central outcome of this study (4.1) shows that the systematic uncertainties in the dispersive representation can be controlled at a level that renders this approach a valuable complementary perspective to the direct integration of the experimental data. In particular, it provides the best controlled extrapolation down to the two-pion threshold where data are less precise or just absent. Once possible uncertainties in the energy calibration are taken into account all present data sets can be described in a statistically acceptable way, providing a strong check on their internal consistency. The combination of data sets follows in a straightforward way from the propagation of the uncertainties, up to a small inflation of the final uncertainties by $\sqrt{\chi^2/\text{dof}} \sim 1.1$ in the standard manner. The inclusion of space-like data sets provides a further consistency check and leads to a modest reduction in uncertainty.

As a side-product, we obtained a precise determination of the pion charge radius (5.2), which provides further evidence that the PDG average for $\langle r_\pi^2 \rangle$ needs to be revised. Another issue concerns the mass of the ω , for which it would be important to clarify the origin of the current mismatch between extractions from the 2π and 3π channels.

Acknowledgements

The speaker (P.S.) thanks the conveners of the CD18 Goldstone-Boson working group for the invitation. Financial support by the DOE (Grants No. DE-FG02-00ER41132 and DE-SC0009919) and the Swiss National Science Foundation (Project No. P300P2_167751) is gratefully acknowledged.

References

- [1] F. Jegerlehner and A. Nyffeler, *The muon $g - 2$* , *Phys. Rept.* **477** (2009) 1 [0902.3360].
- [2] J. Prades, E. de Rafael and A. Vainshtein, *The hadronic light-by-light scattering contribution to the muon and electron anomalous magnetic moments*, *Adv. Ser. Direct. High Energy Phys.* **20** (2009) 303 [0901.0306].
- [3] M. Benayoun et al., *Hadronic contributions to the muon anomalous magnetic moment Workshop. $(g - 2)_\mu$: Quo vadis? Workshop. Mini proceedings*, 1407.4021.
- [4] B. Ananthanarayan, G. Colangelo, J. Gasser and H. Leutwyler, *Roy equation analysis of $\pi\pi$ scattering*, *Phys. Rept.* **353** (2001) 207 [hep-ph/0005297].
- [5] R. García-Martín, R. Kamiński, J. R. Peláez, J. Ruiz de Elvira and F. J. Ynduráin, *The Pion-pion scattering amplitude. IV: Improved analysis with once subtracted Roy-like equations up to 1100 MeV*, *Phys. Rev.* **D83** (2011) 074004 [1102.2183].
- [6] I. Caprini, G. Colangelo and H. Leutwyler, *Regge analysis of the $\pi\pi$ scattering amplitude*, *Eur. Phys. J.* **C72** (2012) 1860 [1111.7160].
- [7] S. M. Roy, *Exact integral equation for pion pion scattering involving only physical region partial waves*, *Phys. Lett.* **36B** (1971) 353.
- [8] J. F. de Trocóniz and F. J. Ynduráin, *Precision determination of the pion form-factor and calculation of the muon $g - 2$* , *Phys. Rev.* **D65** (2002) 093001 [hep-ph/0106025].
- [9] H. Leutwyler, *Electromagnetic form factor of the pion*, in: *Continuous advances in QCD 2002*, eds. K. A. Olive, M. A. Shifman, and M. B. Voloshin, World Scientific, Singapore, pp. 23–40 (2003) [hep-ph/0212324].
- [10] G. Colangelo, *Hadronic contributions to a_μ below one GeV*, *Nucl. Phys. Proc. Suppl.* **131** (2004) 185 [hep-ph/0312017].
- [11] J. F. de Trocóniz and F. J. Ynduráin, *The hadronic contributions to the anomalous magnetic moment of the muon*, *Phys. Rev.* **D71** (2005) 073008 [hep-ph/0402285].
- [12] B. Ananthanarayan, I. Caprini, D. Das and I. Sentitemsu Imsong, *Two-pion low-energy contribution to the muon $g - 2$ with improved precision from analyticity and unitarity*, *Phys. Rev.* **D89** (2014) 036007 [1312.5849].
- [13] B. Ananthanarayan, I. Caprini, D. Das and I. Sentitemsu Imsong, *Precise determination of the low-energy hadronic contribution to the muon $g - 2$ from analyticity and unitarity: An improved analysis*, *Phys. Rev.* **D93** (2016) 116007 [1605.00202].
- [14] M. Hoferichter, B. Kubis, J. Ruiz de Elvira, H.-W. Hammer and U.-G. Meißner, *On the $\pi\pi$ continuum in the nucleon form factors and the proton radius puzzle*, *Eur. Phys. J.* **A52** (2016) 331 [1609.06722].
- [15] C. Hanhart, S. Holz, B. Kubis, A. Kupść, A. Wirzba and C. W. Xiao, *The branching ratio $\omega \rightarrow \pi^+\pi^-$ revisited*, *Eur. Phys. J.* **C77** (2017) 98 [1611.09359].
- [16] M. Hoferichter, G. Colangelo, M. Procura and P. Stoffer, *Virtual photon-photon scattering*, *Int. J. Mod. Phys. Conf. Ser.* **35** (2014) 1460400 [1309.6877].
- [17] G. Colangelo, M. Hoferichter, M. Procura and P. Stoffer, *Dispersive approach to hadronic light-by-light scattering*, *JHEP* **09** (2014) 091 [1402.7081].
- [18] G. Colangelo, M. Hoferichter, B. Kubis, M. Procura and P. Stoffer, *Towards a data-driven analysis of hadronic light-by-light scattering*, *Phys. Lett.* **B738** (2014) 6 [1408.2517].
- [19] G. Colangelo, M. Hoferichter, M. Procura and P. Stoffer, *Dispersion relation for hadronic light-by-light scattering: theoretical foundations*, *JHEP* **09** (2015) 074 [1506.01386].

- [20] G. Colangelo, M. Hoferichter, M. Procura and P. Stoffer, *Rescattering effects in the hadronic-light-by-light contribution to the anomalous magnetic moment of the muon*, *Phys. Rev. Lett.* **118** (2017) 232001 [1701.06554].
- [21] G. Colangelo, M. Hoferichter, M. Procura and P. Stoffer, *Dispersion relation for hadronic light-by-light scattering: two-pion contributions*, *JHEP* **04** (2017) 161 [1702.07347].
- [22] M. Hoferichter, B.-L. Hoid, B. Kubis, S. Leupold and S. P. Schneider, *Pion-pole contribution to hadronic light-by-light scattering in the anomalous magnetic moment of the muon*, *Phys. Rev. Lett.* **121** (2018) 112002 [1805.01471].
- [23] M. Hoferichter, B.-L. Hoid, B. Kubis, S. Leupold and S. P. Schneider, *Dispersion relation for hadronic light-by-light scattering: pion pole*, *JHEP* **10** (2018) 141 [1808.04823].
- [24] G. Colangelo, *Dispersive approach to the hadronic light-by-light contribution to the muon $g - 2$* , in *these proceedings*, PoS (CD2018) 002, 2019.
- [25] F. Jegerlehner, *Muon $g - 2$ theory: the hadronic part*, *EPJ Web Conf.* **166** (2018) 00022 [1705.00263].
- [26] M. Davier, A. Hoecker, B. Malaescu and Z. Zhang, *Reevaluation of the hadronic vacuum polarisation contributions to the Standard Model predictions of the muon $g - 2$ and $\alpha(m_Z^2)$ using newest hadronic cross-section data*, *Eur. Phys. J.* **C77** (2017) 827 [1706.09436].
- [27] A. Keshavarzi, D. Nomura and T. Teubner, *The muon $g - 2$ and $\alpha(M_Z^2)$: a new data-based analysis*, *Phys. Rev.* **D97** (2018) 114025 [1802.02995].
- [28] BABAR collaboration, *Precise measurement of the $e^+e^- \rightarrow \pi^+\pi^-(\gamma)$ cross section with the initial-state radiation method at BABAR*, *Phys. Rev. Lett.* **103** (2009) 231801 [0908.3589].
- [29] BABAR collaboration, *Precise measurement of the $e^+e^- \rightarrow \pi^+\pi^-(\gamma)$ cross section with the initial-state radiation method at BABAR*, *Phys. Rev.* **D86** (2012) 032013 [1205.2228].
- [30] KLOE collaboration, *Measurement of $\sigma(e^+e^- \rightarrow \pi^+\pi^-\gamma(\gamma))$ and the dipion contribution to the muon anomaly with the KLOE detector*, *Phys. Lett.* **B670** (2009) 285 [0809.3950].
- [31] KLOE collaboration, *Measurement of $\sigma(e^+e^- \rightarrow \pi^+\pi^-)$ from threshold to 0.85 GeV^2 using initial state radiation with the KLOE detector*, *Phys. Lett.* **B700** (2011) 102 [1006.5313].
- [32] KLOE collaboration, *Precision measurement of $\sigma(e^+e^- \rightarrow \pi^+\pi^-\gamma)/\sigma(e^+e^- \rightarrow \mu^+\mu^-\gamma)$ and determination of the $\pi^+\pi^-$ contribution to the muon anomaly with the KLOE detector*, *Phys. Lett.* **B720** (2013) 336 [1212.4524].
- [33] KLOE-2 collaboration, *Combination of KLOE $\sigma(e^+e^- \rightarrow \pi^+\pi^-\gamma(\gamma))$ measurements and determination of $a_\mu^{\pi^+\pi^-}$ in the energy range $0.10 < s < 0.95 \text{ GeV}^2$* , *JHEP* **03** (2018) 173 [1711.03085].
- [34] G. Colangelo, M. Hoferichter and P. Stoffer, *Two-pion contribution to hadronic vacuum polarization*, *JHEP* **02** (2019) 006 [1810.00007].
- [35] J. Gluza, A. Hofer, S. Jadach and F. Jegerlehner, *Measuring the FSR inclusive $\pi^+\pi^-$ cross section*, *Eur. Phys. J.* **C28** (2003) 261 [hep-ph/0212386].
- [36] H. Czyż, A. Grzebińska, J. H. Kühn and G. Rodrigo, *The radiative return at ϕ - and B -factories: FSR for muon pair production at next-to-leading order*, *Eur. Phys. J.* **C39** (2005) 411 [hep-ph/0404078].
- [37] Y. M. Bystritskiy, E. A. Kuraev, G. V. Fedotovitch and F. V. Ignatov, *The Cross sections of the muons and charged pions pairs production at electron-positron annihilation near the threshold*, *Phys. Rev.* **D72** (2005) 114019 [hep-ph/0505236].

- [38] G. Rodrigo, H. Czyż, J. H. Kühn and M. Szopa, *Radiative return at NLO and the measurement of the hadronic cross-section in electron positron annihilation*, *Eur. Phys. J.* **C24** (2002) 71 [[hep-ph/0112184](#)].
- [39] H. Czyż, A. Grzebińska, J. H. Kühn and G. Rodrigo, *The radiative return at ϕ - and B-factories: small angle photon emission at next-to-leading order*, *Eur. Phys. J.* **C27** (2003) 563 [[hep-ph/0212225](#)].
- [40] H. Czyż, A. Grzebińska, J. H. Kühn and G. Rodrigo, *The radiative return at ϕ - and B-factories: FSR at next-to-leading order*, *Eur. Phys. J.* **C33** (2004) 333 [[hep-ph/0308312](#)].
- [41] R. Omnès, *On the solution of certain singular integral equations of quantum field theory*, *Nuovo Cim.* **8** (1958) 316.
- [42] L. Łukaszuk, *A generalization of the Watson theorem*, *Phys. Lett.* **47B** (1973) 51.
- [43] S. Eidelman and L. Łukaszuk, *Pion form-factor phase, $\pi\pi$ elasticity and new e^+e^- data*, *Phys. Lett.* **B582** (2004) 27 [[hep-ph/0311366](#)].
- [44] K. M. Watson, *Some general relations between the photoproduction and scattering of π mesons*, *Phys. Rev.* **95** (1954) 228.
- [45] M. N. Achasov et al., *Study of the process $e^+e^- \rightarrow \pi^+\pi^-$ in the energy region $400 < \sqrt{s} < 1000$ MeV*, *J. Exp. Theor. Phys.* **101** (2005) 1053 [[hep-ex/0506076](#)].
- [46] M. N. Achasov et al., *Update of the $e^+e^- \rightarrow \pi^+\pi^-$ cross section measured by SND detector in the energy region $400\text{MeV} < \sqrt{s} < 1000\text{MeV}$* , *J. Exp. Theor. Phys.* **103** (2006) 380 [[hep-ex/0605013](#)].
- [47] CMD-2 collaboration, *Measurement of $e^+e^- \rightarrow \pi^+\pi^-$ cross section with CMD-2 around ρ meson*, *Phys. Lett.* **B527** (2002) 161 [[hep-ex/0112031](#)].
- [48] CMD-2 collaboration, *Reanalysis of hadronic cross-section measurements at CMD-2*, *Phys. Lett.* **B578** (2004) 285 [[hep-ex/0308008](#)].
- [49] R. R. Akhmetshin et al., *Measurement of the $e^+e^- \rightarrow \pi^+\pi^-$ cross section with the CMD-2 detector in the 370 – 520 MeV c.m. energy range*, *JETP Lett.* **84** (2006) 413 [[hep-ex/0610016](#)].
- [50] CMD-2 collaboration, *High-statistics measurement of the pion form factor in the rho-meson energy range with the CMD-2 detector*, *Phys. Lett.* **B648** (2007) 28 [[hep-ex/0610021](#)].
- [51] NA7 collaboration, *A measurement of the space-like pion electromagnetic form factor*, *Nucl. Phys.* **B277** (1986) 168.
- [52] NNPDF collaboration, *Fitting parton distribution data with multiplicative normalization uncertainties*, *JHEP* **05** (2010) 075 [[0912.2276](#)].
- [53] G. D’Agostini, *On the use of the covariance matrix to fit correlated data*, *Nucl. Instrum. Meth.* **A346** (1994) 306.
- [54] M. N. Achasov et al., *Study of the process $e^+e^- \rightarrow \pi^+\pi^-\pi^0$ in the energy region \sqrt{s} below 0.98 GeV*, *Phys. Rev.* **D68** (2003) 052006 [[hep-ex/0305049](#)].
- [55] PARTICLE DATA GROUP collaboration, *Review of particle physics*, *Phys. Rev.* **D98** (2018) 030001.
- [56] B. Ananthanarayan, I. Caprini and D. Das, *Pion electromagnetic form factor at high precision with implications to $a_\mu^{\pi\pi}$ and the onset of perturbative QCD*, *Phys. Rev.* **D98** (2018) 114015 [[1810.09265](#)].
- [57] B. Ananthanarayan, I. Caprini and D. Das, *Electromagnetic charge radius of the pion at high precision*, *Phys. Rev. Lett.* **119** (2017) 132002 [[1706.04020](#)].
- [58] C. J. Bebek et al., *Electroproduction of single pions at low ϵ and a measurement of the pion form factor up to $Q^2 = 10\text{GeV}^2$* , *Phys. Rev.* **D17** (1978) 1693.
- [59] A1 collaboration, *A measurement of the axial form factor of the nucleon by the $p(e, e'\pi^+)n$ reaction at $W = 1125\text{MeV}$* , *Phys. Lett.* **B468** (1999) 20 [[nucl-ex/9911003](#)].